

Y.-C. N. Cheng
T. P. Eagan
T. Chmielewski
J. Flock
M.-C. Kang
T. K. Kidane
Sh. M. Shvartsman
R. W. Brown

A degeneracy study in the circulant and bordered-circulant approach to birdcage and planar coils

Received: 17 October 2002
Accepted: 24 February 2003
Published online: 25 July 2003
© ESMRMB 2003

Y.-C. N. Cheng · T. P. Eagan
T. K. Kidane · S. M. Shvartsman
R. W. Brown (✉)
Department of Physics,
Case Western Reserve University,
Cleveland, Ohio 44106, USA
e-mail: rwb@po.cwru.edu
Tel.: +1-216-368-4010
Fax: +1-216-368-4671

T. Chmielewski · J. Flock
S. M. Shvartsman
Magnetic Resonance Division,
Philips Medical Systems (Cleveland) Inc.,
Highland Heights, Ohio 44143, USA

M.-C. Kang
Department of Mathematics,
National Taiwan University,
Taipei, Taiwan, ROC

Abstract A method for finding closed-form solutions for the normal mode frequencies of systems with circulant $\left(\frac{2\pi}{n}\right)$ symmetry was investigated. This method is particularly useful for questions of degeneracy that arise when one considers parallel imaging techniques like SENSE and SMASH in MRI. It is applicable to systems that include birdcage coils as well as planar coils with the appropriate rotational symmetry. A proof is given that complete degeneracy of all normal mode frequencies is impossible when all mutual inductive couplings are included. We tested the method against measurements made on a planar coil array and on an 8-element birdcage coil. The inclusion of the co-rotating end-ring

mode changes the fundamental symmetry of the system from circulant to ‘bordered circulant.’ Closed-form solutions for the normal mode frequencies of a bordered circulant system are also given.

Keywords RF coils · Analytic solutions · Circulant

Introduction

Several techniques exist for determining the normal mode frequencies of the resonant circuits typically found in the RF subsystem of modern MR scanners. [1, 2, 3]. While these numerical methods are quite useful in practice, one also may make good progress using analytic solutions. For certain geometries, it is possible to find closed-form solutions for normal mode frequencies. While some earlier work [2, 4, 5] considered only nearest-neighbor couplings, Leifer [6] has included all couplings in a ‘circulant’ approach [6] and closed-form solutions were found for birdcage coils. In the present paper, we have expanded the approach for coils having ‘circulant symmetry’ (to be defined). Some of the

results of our work have already been discussed in [7, 8].

These closed-form solutions are particularly valuable because of the current interest in degenerate normal mode frequency spectra in SENSE and SMASH studies. [9, 10]. For the case of SMASH, it is straightforward to find a set of weightings such that sinusoidal field variations are approximated [10]. This process, however, makes the key assumption that all the normal mode frequencies are degenerate. Another approach to the degeneracy question is to design a coil that has an inherently sinusoidal field variation mode as well as a uniform field mode, then tune it such that these modes are degenerate [11, 12, 13]. There are several techniques using different forms of electronic decoupling to achieve degeneracy in

practice. Some examples of these techniques include those described in [14, 15, 16]. In an example discussed below, one specific form of electronic decoupling, namely, capacitive decoupling, is utilized.

The question of degeneracy has been previously addressed by [4, 5, 17, 18]. The approach discussed in this paper is quite effective in determining the normal mode frequencies and in understanding, in particular, the circumstances in which degeneracy is impossible. We will present a general ‘impossibility’ proof for complete degeneracy, thus limiting the maximum number of degenerate normal modes. It is important to note that the closed-form solutions investigated here are of value in general, not just in the context of questions of degeneracy.

In the typical analysis of a birdcage coil, one of the modes (the so-called co-rotating end-ring mode) is usually ignored because it does not produce significant field components in the transverse plane [2]. We will also find a closed-form solution for a birdcage including this mode using the notion of a ‘bordered circulant.’ The normal modes and frequencies will be compared to the results for the case when the co-rotating mode is ignored.

The analysis used for both the systems with circulant and bordered circulant symmetry neglects loss in both the coil and the coil load. The loss in the system can be separated into two parts: the loss due to the small resistance in the coil copper strips and that due to the sample resistance. It is reasonable to assume that the loss in the coil strips has circulant symmetry and therefore we may still derive closed-form expressions. The inclusion of the sample loss in the model is not as straightforward. The details of the shape and internal structure of the sample need to be taken into consideration, making it unlikely that the resulting Kirchhoff’s law impedance matrix has circulant symmetry. We call attention to the fact that, although for any real coil the losses are nonzero, we have been able to completely neglect the loss in the system and still have good agreement with experiments. Successful comparisons have been made between the theoretical frequency spectrum and that experimentally measured for a planar array coil and a birdcage coil constructed for testing purposes.

Methods and discussion

Circulant theory

An $n \times n$ matrix has ‘circulant’ symmetry when each row is a cyclic permutation of the previous row, such as:

$$A = \begin{pmatrix} a_1 & a_2 & \dots & a_n \\ a_n & a_1 & a_2 & \dots \\ \vdots & \vdots & \vdots & \vdots \\ \dots & a_n & a_1 & a_2 \\ a_2 & \dots & a_n & a_1 \end{pmatrix} \quad (1)$$

In this case, its determinant can be written in a powerfully simple form [19] that follows directly from the ability to diagonalize the matrix A as is given by:

$$\text{Det}(A) = \prod_{j=0}^{n-1} \left(\sum_{k=1}^n a_k e^{i2\pi \left(\frac{j(k-1)}{n} \right)} \right) \quad (2)$$

Let us examine how one arrives at Eq. 2. There exists a unitary transformation that diagonalizes Eq. 1:

$$U^\dagger A U = \begin{pmatrix} u_1 & 0 & \dots & 0 \\ 0 & u_2 & \dots & 0 \\ & & \ddots & \\ 0 & \dots & 0 & u_n \end{pmatrix} \quad (3)$$

A unitary matrix that diagonalizes the circulant matrix can be represented in terms of the n -roots of one, $\gamma = e^{\frac{i2\pi}{n}}$,

$$U = \frac{1}{\sqrt{n}} \begin{pmatrix} 1 & 1 & 1 & \dots & 1 \\ 1 & \gamma & \gamma^2 & \dots & \gamma^{n-1} \\ 1 & \gamma^2 & \gamma^4 & \dots & \gamma^{2(n-1)} \\ \vdots & \vdots & \vdots & \dots & \vdots \\ 1 & \gamma^{(n-1)} & \gamma^{2(n-1)} & \dots & \gamma^{(n-1)(n-1)} \end{pmatrix} \quad (4)$$

With U given by Eq. 4 and A given by Eq. 1, it follows that the diagonal elements of the matrix in Eq. 3 are given by $u_j = \sum_{k=1}^n a_k e^{i2\pi \left(\frac{(j-1)(k-1)}{n} \right)}$. In the diagonal form, the determinant is a trivial calculation and it is clear the form given in Eq. 2 is recovered, recalling that $\text{Det}(U^\dagger A U) = \text{Det}(A)$.

The presence of mirror planes in the system results in a matrix with an additional symmetry. The matrix representation of a system with circulant symmetry as well as mirror planes is given by:

$$\tilde{A} = \begin{pmatrix} a_1 & a_2 & a_3 & \dots & a_3 & a_2 \\ a_2 & a_1 & a_2 & a_3 & \dots & a_3 \\ a_3 & a_2 & a_1 & a_2 & a_3 & \dots \\ \vdots & \vdots & \vdots & \vdots & \vdots & \vdots \\ a_2 & a_3 & \dots & a_3 & a_2 & a_1 \end{pmatrix} \quad (5)$$

This allows the determinant to be written in the following form:

$$\text{Det}(\tilde{A}) = \prod_{j=0}^{n-1} \left(\sum_{k=1}^n \cos \left(2\pi j \frac{k-1}{n} \right) a_k \right) \quad (6)$$

Both these forms should remind the reader of the discrete Fourier transformation (see the remarks in [6]).

The reason for interest in the determinant of a matrix of the forms discussed above is that matrices such as A and \tilde{A} are found in the circuit equations for systems like the birdcage. Kirchhoff’s laws may be written in matrix form as:

$$A I = 0 \quad (7)$$

The matrix elements of A_{ij} are proportional to the *emf* drops in the i^{th} loop associated with the current in the j^{th} loop. Let ω denote the normal mode frequency. The general form of the impedances due to the self-inductive term is $i\omega L$, the mutual inductive form is $i\omega M$, and the capacitive form is $\frac{1}{i\omega c}$ assuming the current in the system has an $e^{i\omega t}$ time dependence.

The normal mode frequencies are found by solving $\text{Det}(A)=0$ or $\text{Det}(\tilde{A})=0$. The closed-form solutions given above have automatically factored the general $(2n)^{\text{th}}$ -order polynomial into a product of n quadratic polynomials in the normal mode frequencies, ω . Solving for the frequencies is now much easier, and in practice all solutions can be found in closed form. This technique has been used in the present paper to find the normal mode frequencies of all problems involving $\frac{2\pi}{n}$ symmetric structures. In contrast, determining the roots of the original $(2n)^{\text{th}}$ -order polynomial using numerical techniques such as Newton's method can be computationally expensive and may in some case need very high precision to find the root accurately. We have found it necessary to use GNU-MP, a C-library for arbitrary precision arithmetic. For the root-finding algorithm to produce results that agree with the analytic results to double precision, it was necessary to keep at least 60 digits of precision while calculating the determinant. Keeping this large amount of precision slows down the code greatly; it also produces code that is much more cumbersome. In practice, on a five-loop example the arbitrary precision code took about a weekend to run while the code that evaluated the analytic expressions was instantaneous. Thus, it is clear that closed-form solutions significantly reduce the amount of computing power required to find the normal mode frequencies.

We may illustrate the difference in finding the roots of a determinant. With closed-form solutions, the zeros of an N^{th} -order polynomial are an $O(N)$ problem. An it-

$$\hat{A} = \begin{pmatrix} L - \frac{1}{w^2 C_{1eff}} & M_{\text{near}} - \frac{1}{w^2 C_{2eff}} & M_{\text{far}} & M_{\text{near}} - \frac{1}{w^2 C_{2eff}} \\ M_{\text{near}} - \frac{1}{w^2 C_{2eff}} & L - \frac{1}{w^2 C_{1eff}} & M_{\text{near}} - \frac{1}{w^2 C_{2eff}} & M_{\text{far}} \\ M_{\text{far}} & M_{\text{near}} - \frac{1}{w^2 C_{2eff}} & L - \frac{1}{w^2 C_{1eff}} & M_{\text{near}} - \frac{1}{w^2 C_{2eff}} \\ M_{\text{near}} - \frac{1}{w^2 C_{2eff}} & M_{\text{far}} & M_{\text{near}} - \frac{1}{w^2 C_{2eff}} & L - \frac{1}{w^2 C_{1eff}} \end{pmatrix} \quad (12)$$

erative approach for factoring this polynomial is at least $O(N^2)$. Other numerical methods that do not involve this determinant calculation may be faster, of course. However, none can be expected to better an $O(N)$ method.

Exact degeneracy of all frequencies

Starting from Kirchoff's law given by Eq. 7, we may examine the possibility of having complete degeneracy of all normal mode frequencies of any resonant circuit.

Defining the matrix $\hat{A} = \frac{A}{i\omega}$, we see that it is real and symmetric which is a special case of Hermiticity. For any Hermitian matrix, there exists a unitary transformation that diagonalizes \hat{A} . Thus Eq. 7 may be rewritten as:

$$(\hat{U}^\dagger \hat{A} \hat{U}) (\hat{U}^\dagger I) = B I' = 0 \quad (8)$$

where

$$B = \begin{pmatrix} \lambda_1(\omega) & 0 & 0 \\ 0 & \ddots & \vdots \\ 0 & \dots & \lambda_1(\omega) \end{pmatrix} \quad (9)$$

The matrix B is diagonal and the diagonal values B_{ii} are its eigenvalues, λ_i , and are a function of the same parameters that appear in \hat{A} . Complete degeneracy requires all eigenvalues to be the same. The additional constraint that Eq. 8 be satisfied for nontrivial I' implies that B is a zero matrix:

$$B = \begin{pmatrix} 0 & \dots & 0 \\ \vdots & \ddots & \vdots \\ 0 & \dots & 0 \end{pmatrix} \quad (10)$$

The inverse unitary transformation takes us back to the original basis, revealing that \hat{A} must therefore have the same null form:

$$\hat{A} = \hat{U} B \hat{U}^\dagger = \begin{pmatrix} 0 & \dots & 0 \\ \vdots & \ddots & \vdots \\ 0 & \dots & 0 \end{pmatrix} \quad (11)$$

However, there is a fundamental contradiction here. If we consider a four axial-element birdcage, the matrix \hat{A} has the following form:

We consider this coil as the simplest birdcage in which next-nearest-neighbor coupling is important. The obstacle to degeneracy posed by the next-nearest neighbors is now evident. Notice there are no capacitive terms to cancel the M_{far} term of the matrix \hat{A} . For certain geometries, one may be able to contrive a situation in which M_{far} is zero. However, M_{far} is typically nonzero and for this case exact degeneracy is impossible. This situation is attained

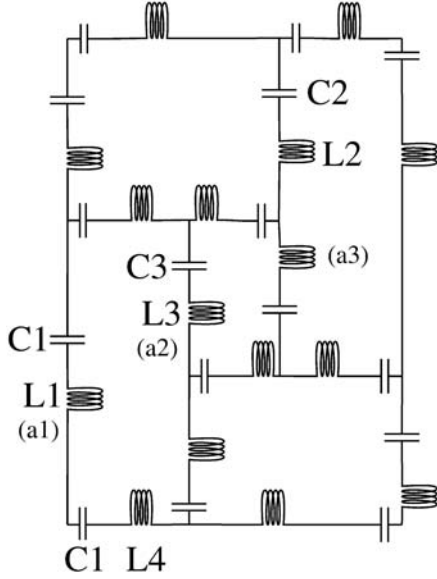


Fig. 1 Small decoupling loop embedded in a four-loop square. Degeneracy of four modes can be achieved with the additional degrees of freedom of the small loop

for any lattice of loops for which inductive couplings beyond nearest-neighbor (loops that share a common leg) are considered. In the example above, the effects of loading the coil have been neglected. However, it is still impossible to obtain a zero matrix when the load is included. This can most easily be understood by realizing that the addition of a real impedance cannot cancel the imaginary term corresponding to M_{far} , which was described previously.

Simple system

Before we apply the results from circulant theory to our modeling, let us examine a simple system for which closed-form solutions are readily achievable. Consider a planar array as shown in Fig. 1. Note that this coil is topologically equivalent to a four-rung (four axial-element) birdcage. That is, one can continuously deform one coil into the other. We have been able to show analytically that there exists a solution with four identically degenerate frequencies in this five-loop array. A previous study has demonstrated experimentally that a similar five-loop array has multiple degenerate frequencies [17]. Note this does not contradict the unitary matrix proof that was offered in the previous section; that proof leads to the impossibility of *all* normal-mode frequencies being equal in such coils. In the present case, one frequency differs from the other four. It is associated with the small ('parasitic') central coil.

We briefly outline the analytic work behind this progress. An experimental verification is described after-

ward. The matrix A in Eq. 7 for the circuit in Fig. 1 can be written as:

$$\begin{pmatrix} m_3 - \alpha & m_4 + \frac{1}{C_2 w^2} & m_5 & m_4 + \frac{1}{C_2 w^2} & m_2 + \frac{1}{C_3 w^2} \\ m_4 + \frac{1}{C_2 w^2} & m_3 - \alpha & m_4 + \frac{1}{C_2 w^2} & m_5 & m_2 + \frac{1}{C_3 w^2} \\ m_5 & m_4 + \frac{1}{C_2 w^2} & m_3 - \alpha & m_4 + \frac{1}{C_2 w^2} & m_2 + \frac{1}{C_3 w^2} \\ m_4 + \frac{1}{C_2 w^2} & m_5 & m_4 + \frac{1}{C_2 w^2} & m_3 - \alpha & m_2 + \frac{1}{C_3 w^2} \\ m_2 + \frac{1}{C_3 w^2} & m_2 + \frac{1}{C_3 w^2} & m_2 + \frac{1}{C_3 w^2} & m_2 + \frac{1}{C_3 w^2} & m_1 + \frac{1}{C_3 w^2} \end{pmatrix} \quad (13)$$

$$\text{where } \alpha \equiv \frac{2}{C_1 w^2} - \frac{2}{C_2 w^2} - \frac{1}{C_3 w^2}.$$

The five normal-mode frequencies of the system are found by using Mathematica's analytical tools (for finding the roots of a fifth-order polynomial in $\frac{1}{w^2}$ and the results are

$$w_1 = \frac{1}{\sqrt{\frac{C_1 C_2 C_3 (m_3 - m_5)}{C_1 C_2 + 2(C_1 + C_2) C_3}}} \quad (14)$$

$$w_2 = \frac{1}{\sqrt{\frac{C_1 C_2 C_3 (m_3 - m_5)}{C_1 C_2 + 2(C_1 + C_2) C_3}}} \quad (15)$$

$$w_3 = \frac{1}{\sqrt{\frac{C_1 C_2 C_3 (m_3 - 2m_4 + m_5)}{2C_2 C_3 + C_1 (C_2 + 4C_3)}}} \quad (16)$$

$$w_4 = \frac{4}{\sqrt{2C_3 m_1 + C_1 (m_1 + 4(2m_2 + m_3 + 2m_4 + m_5)) - \beta}} \quad (17)$$

$$w_5 = \frac{4}{\sqrt{2C_3 m_1 + C_1 (m_1 + 4(2m_2 + m_3 + 2m_4 + m_5)) + \beta}} \quad (18)$$

where m_i are effective inductances given by:

$$m_1 = 4L_3 - 4M_{33} \quad (19)$$

$$m_2 = -L_3 + M_{13c} - M_{13f} + M_{34c} - M_{34f} + M_{33} \quad (20)$$

$$m_3 = L_1 + L_4 + 2L_2 + L_3 - 2M_{12c} - 2M_{13c} - 2M_{24f} + 2M_{23c} \quad (21)$$

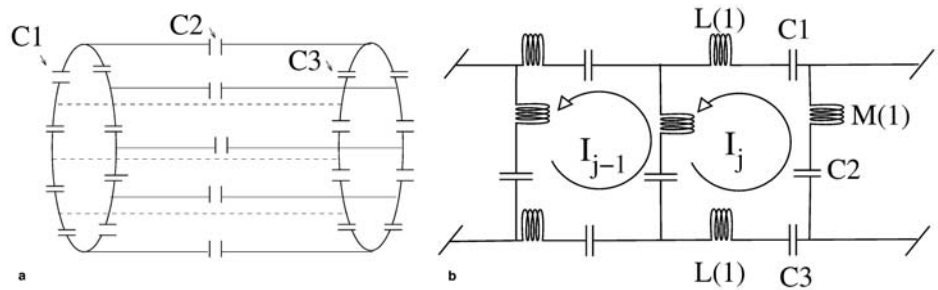
$$m_4 = -L_2 - M_{14c} + M_{14f} + M_{12c} - M_{12f} - M_{24c} + M_{24f} - M_{34c} + M_{34f} + M_{22} - M_{23c} + M_{23f} \quad (22)$$

$$m_5 = -M_{11} + 2M_{12f} + 2M_{13f} - M_{44} + 2M_{24c} - 2M_{22} - 2M_{23f} - M_{33} \quad (23)$$

and the self-inductances are defined in Fig. 1. M_{ij} is the mutual inductance between the i^{th} and j^{th} circuit elements and c and f refer to 'close' and 'far.' For instance, the coupling between segments a1 and a2 in Fig. 1 would be denoted M_{13c} and between segments a1 and a3 would be denoted M_{13f} . The quantity β is defined to

$$\text{be } \beta = \sqrt{-32C_1 C_3 (-4m_2^2 + m_1 (m_3 + 2m_4 + m_5))} + \Gamma, \text{ with } \Gamma = (2C_3 m_1 + C_1 (m_1 + 4(2m_2 + m_3 + 2m_4 + m_5)))^2.$$

Fig. 2 **a** A typical bandpass birdcage with complete circulant symmetry. **b** The concomitant circuit diagram for this birdcage



Through further use of Mathematica's analytical tools, the values of C_1 and C_3 have been found such that four of the five normal-modes are degenerate. They are:

$$C_1 = \frac{-2(C_2C_3m_4 - C_2C_3m_5)}{C_3m_3 + C_2m_4 + 2C_3m_4 - C_2m_5 - 3C_3m_5} \quad (24)$$

$$C_3 = \frac{2C_2m_2m_4 - 2C_2m_2m_5 + 4C_2m_4m_5 - 4C_2m_5^2 - \Delta}{2(m_2^2 - m_1m_5)} \quad (25)$$

$$\Delta = 2C_2(m_4 - m_5) \sqrt{m_5(m_1 + 4m_2 + 4m_5)} \quad (26)$$

The last capacitance value C_2 may be adjusted to give the desired overall frequency scale.

To test the analysis, an experimental 'square-pin-wheel' coil was constructed according to Fig. 1 with the length of the side for the larger square being 30 cm and for the smaller square being 5 cm. All conductors are made of copper tape with a rectangular cross-section of 1.0 cm×0.009 cm. From the theoretical formulas and the constraint that the scale of the degenerate frequency match a 1.5-Tesla Larmor precession frequency, the capacitors on the outside square were found to be $C_1=50$ pF. The capacitors on the inside and the capacitors on the legs that connected the outside to the inside were determined to be $C_3=130$ pF and $C_2=102.2$ pF, respectively. Experimental measurements led to four normal-mode frequencies lying between 62.3 MHz and 63.4 MHz and a fifth mode at 84.9 MHz. This is in excellent agreement with the predicted values of four degenerate modes at 63.7 MHz and the fifth mode at 90 MHz, particularly in view of the uncertainties represented by the capacitor tolerance and the stray inductance associated with the capacitance attachment.

A near-degenerate circulant 8-rung birdcage

Although perfect degeneracy is not possible, we consider the construction of a birdcage with 'cage' modes that are almost degenerate. We apply the results from the determinant of a circulant matrix to find nearly degenerate normal mode frequencies of an 8-rung birdcage. These theoretical results are then compared to experiment. A coil of radius 11.74 cm and axial length of 24.5 cm

was both constructed and theoretically modeled with $C_1=C_3=59.8$ pF and $C_2=49.2$ pF as depicted in Fig. 2. Copper tape was again used with rectangular cross-section dimensions 1.0 cm×0.009 cm in both the model and the construction. Using the closed form from the determinant of a circulant matrix, the calculation results for the normal mode frequencies yielded very good agreement with the experimental data. The matrix A is an 8×8 matrix that is a symmetric matrix which has 36 independent matrix elements. The details of this calculation are similar to those discussed in the previous section on the square-pinwheel coil and can be found in Appendix A. The magnitude of the inductive couplings were determined by numerical integration. Using the dimensions and capacitive values given above, the normal mode frequencies of the seven cage modes were determined to be in the range 63.42 MHz to 64.66 MHz. The end-ring mode was calculated to resonate at 76 MHz.

A typical bandpass birdcage was constructed and a range of the capacitance values were studied to achieve near degeneracy. The normal mode frequencies of the seven cage modes were found via a 'two-loop coupled flux measurement' to vary from 65.26 MHz to 66.74 MHz. The end-ring-mode was found to be at approximately 76 MHz. The values of C_1 and C_2 were found experimentally to minimize the spread in frequencies of the seven cage modes (1.48 MHz in the above case). Note that one could not use the capacitance/inductance relations given in the references [4, 5] owing to the importance of the non-nearest-neighbor couplings.

Extra mode for the birdcage

Many standard treatments of the birdcage tend to ignore one of the normal modes on the grounds that it produces a field that is not predominantly in the transverse plane. However, if one is interested in investigating the use of birdcages in vertical field systems, for instance, this mode may become of more interest and utility. Our concern is finding a closed-form solution for the normal mode frequencies of a system when the 'co-rotating' mode (Fig. 3) is included in the analysis. (A different and simple approach to the extra mode has been discussed previously in [6].) There is an immediate problem

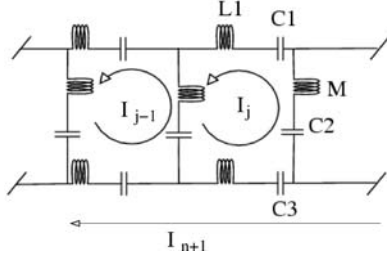


Fig. 3 A circuit diagram for a typical bandpass birdcage with the co-rotating mode labeled

when one writes down Kirchoff's laws including this mode. The matrix A no longer has the circulant symmetry required for the closed-form given in Eq. 1. However, it does have a form known as a bordered circulant. The determinant of this form also has a closed-form expression, to which we now turn our attention.

Bordered circulant

A bordered circulant is a matrix of the form:

$$A = \begin{pmatrix} a_1 & a_2 & \cdots & a_n & y_1' \\ a_n & a_1 & \cdots & a_{n-1} & y_2' \\ \vdots & \vdots & \vdots & \vdots & \vdots \\ a_2 & a_3 & \cdots & a_1 & y_n' \\ y_1 & y_2 & \cdots & y_n & t \end{pmatrix} \quad (27)$$

One can construct a new unitary transformation (U) from the matrix U given in Eq. 4 in which:

$$U = \begin{pmatrix} U & 0 \\ 0 & 1 \end{pmatrix} \quad (28)$$

One now applies this new unitary transformation to A :

$$U^\dagger A U = \begin{pmatrix} u_1 & 0 & 0 & \cdots & 0 & w_1 \\ 0 & u_2 & 0 & & 0 & w_2 \\ \vdots & 0 & \ddots & 0 & \vdots & \vdots \\ 0 & 0 & & u_{n-1} & 0 & w_{n-1} \\ 0 & 0 & \cdots & 0 & u_n & w_n \\ v_1 & v_2 & \cdots & v_{n-1} & v_n & t \end{pmatrix} \quad (29)$$

In this form one can readily verify that by doing the cofactor expansion the determinant of A is given by:

$$\text{Det}(A) = \prod_{i=1}^n u_i \left(t - \sum_{j=1}^n \frac{v_j w_j}{u_j} \right) \quad (30)$$

where

$$\begin{pmatrix} w_1 \\ \vdots \\ w_n \end{pmatrix} = U^\dagger \begin{pmatrix} y_1' \\ \vdots \\ y_n' \end{pmatrix} \quad (31)$$

and $(v_1, \dots, v_n) = (y_1, \dots, y_n)U$. We note that the work presented in the previous section for the planar array coil utilized brute-force factoring. However, as the number of coils increases, the degree of the polynomial that one needs to factor increases. Thus, the brute force method becomes unwieldy. The bordered circulant approach produces the same analytic solutions with an economy of effort.

Let us examine the square-pinwheel coil in the light of the results from the bordered circulant. One of the most significant features that should be noted is that in Eq. 13 all the border elements are the same. This is significant because it forces the vector v to be reduced to the form $v = (\sqrt{n}y_1, 0, \dots, 0)$; by symmetry, the vector w has a similar form. Now, we turn our attention to Eq. 30. With w and v given above, the $\text{Det}(A)$ can be simplified in the following way:

$$\text{Det}(A) = (tu_1 - y_1^2 n) \prod_{i=2}^n u_i \quad (32)$$

An examination of Eq. 32 closely reveals that modes 2 through n are unchanged by the addition of a border of this type. At this point we repeat our observation that the square-pinwheel coil presented in Fig. 1 is topologically equivalent to a four-rung birdcage.

Comparison of n -mode and $n+1$ -mode birdcages

For comparison, a four-rung birdcage coil was built with radius 10.75 cm and an axial length 19.5 cm. Two modes were experimentally measured to resonate at 62.82 MHz and 63.07 MHz for an unloaded coil. The one end-ring capacitor was 20 pF, the other end-ring capacitor was 150 pF, and the axial capacitor was 68 pF. The frequencies were calculated to be 62.87 MHz and 63.59 MHz, in excellent agreement with the experimental values. For the four-mode birdcage with four axial elements, we have calculated the normalized current normal modes and frequencies, as given in Table 1. We note that the modes presented in Table 1 are obtained exactly from closed-form expressions and are good within the accuracy that the impedances are known.

Now let us consider the inclusion of the co-rotating end-ring mode in the theoretical calculations. As noted previously, this changes the fundamental symmetry for the system from circulant to bordered circulant. For the five-mode birdcage (with bordered circulant symmetry) with four axial legs, we have found the normal modes shown in Table 2. The original end-ring mode now splits into two modes (modes 1 and 5 in Table 2). The magnitude of this split is directly related to of the asymmetry between C_1 and C_3 . When $C_1=C_3$, this splitting is minimized; however, in practice, one typically uses either C_1 or C_3 for impedance matching. For the case described above, when the series equivalent capacitance is equally

Table 1 Five-Mode Birdcage: Complete Set of Normal Modes where I1, I2, I3 and I4 are any successive set of loop currents in the birdcage and I5 is the current on one of the end-rings as depicted in Fig. 2b

	Mode 1	Mode 2	Mode 3	Mode 4
f(MHz)	74.43	63.59	63.59	62.87
I1	0.5	0	$\frac{\sqrt{2}}{2}$	-0.5
I2	0.5	$-\frac{\sqrt{2}}{2}$	0	0.5
I3	0.5	0	$-\frac{\sqrt{2}}{2}$	-0.5
I4	0.5	$\frac{\sqrt{2}}{2}$	0	0.5

Table 2 Four-Mode Birdcage: Incomplete Set of Normal Modes where I1, I2, I3 and I4 are any successive set of loop currents in the birdcage as depicted in Fig. 3

	Mode 1	Mode 2	Mode 3	Mode 4	Mode 5
f(MHz)	97.21	63.59	63.59	62.87	35.47
I1	0.4508	0	$\frac{\sqrt{2}}{2}$	-0.5	0.0053
I2	0.4508	$-\frac{\sqrt{2}}{2}$	0	0.5	0.0053
I3	0.4508	0	$-\frac{\sqrt{2}}{2}$	-0.5	0.0053
I4	0.4508	$\frac{\sqrt{2}}{2}$	0	0.5	0.0053
I5	0.4326	0	0	0	0.9999

distributed on both end-ring capacitors, we have $C_1=C_3=35.29$ pF and the split between the co-rotating and counter-rotating mode is 2.55 MHz. In general, the cage modes are unchanged by the inclusion of the co-rotating mode. When $C_1=C_3$, one of the two end-ring mode frequencies is unchanged as well. Thus, it is valid to ignore the additional end-ring mode for situations when both end-ring capacitors are identical. This can easily be understood through Eq. 32 since Kirchoff's laws for a four axial-element birdcage including the co-rotating end-ring have a similar form to those presented for the square-pinwheel coil. In addition, for most applications it is sufficient to consider only the original n -modes used in the model above, because the end-ring modes do not produce a field direction useful for imaging in conventional horizontal-field magnets. This point has been made previously by Jin [2].

Conclusions

We have investigated the utility of closed-form solutions for birdcage coils and other coils with circulant symmetry. These closed-form solutions give insights as to the conditions that lead to degeneracy and the circumstances that cause non-degeneracy. The existence of analytic expressions for the frequencies allows one to more easily minimize the overall spread, or the spread of a subset of frequencies. This is of particular interest in the field of parallel imaging, since one may wish to investigate a coil for both conventional usage as well as 'accelerated' usage. We note also the utility of closed-form solutions for systems with bordered circulant symmetry as well as with circulant symmetry, independent of the number of loops.

As noted previously, having the closed-form solutions impacts directly on the amount of computing power required to find the normal mode frequencies and the associated normal mode currents. Coupled with the expres-

sions for self- and mutual inductances given by Grover [20], it is possible to have solutions for the normal mode frequencies that are functions only of the physical dimensions of the coil and the values of the capacitors in the system. Recall that the circulant symmetry requires a $\frac{2\pi}{n}$ rotational symmetry; this dictates that certain capacitors in the system have a common value. In practice, one does not have capacitors with identical values; however, using capacitors with 5% tolerance we have achieved excellent agreement between theory and experiment.

Acknowledgements This work has been supported by Philips Medical Systems and an NIH R21 RR15211-01 grant. We thank Gordon DeMeester and Wayne Dannels for many helpful discussions.

Appendix A

The matrix element a_i from Eq. 5 is given by:

$$a_1 = \frac{-\delta(1, i)}{w^2 C_{1eff}} + 2\tilde{M}(i) - \tilde{M}(\text{mod}(i-1, n)) - \tilde{M}(\text{mod}(i+1, n)) + 2(L(i) - M_{\text{end}}(i)) \quad (33)$$

and $\tilde{M}(i) = \frac{-\delta(1, i)}{w^2 C_2} + M(i)$. $M(i)$ is the self-inductance of the axial leg for $i=1$ and, for $i \neq 1$, it is the mutual inductance between the first and i^{th} axial element. C_2 is the capacitor on the axial leg. The quantity, C_{1eff} is the series equivalent capacitance on the end ring and is given by $\frac{1}{C_{1eff}} = \frac{1}{C_1} + \frac{1}{C_3}$. $L(i)$ is the self inductance of the end ring segment for $i=1$ and, for $i \neq 1$, it is the mutual inductance between the first and i^{th} end ring segments for both segments on the same end ring. $M_{\text{end}}(i)$ is the mutual inductance between the first and i^{th} end ring segments on the opposing end ring. The quantity $\text{mod}(k, n)$ is defined to be the remainder of division of k by n . The analytic expressions for the frequencies are:

$$f_1 = \frac{\sqrt{C_{1eff} + \frac{C_2}{2}}}{2\pi\sqrt{C_{1eff}C_2\alpha}} \quad (34)$$

$$f_2 = \frac{\sqrt{C_{1eff} + \frac{C_2}{2}}}{2\pi\sqrt{C_{1eff}C_2\alpha}} \quad (35)$$

$$f_3 = \frac{1}{2\pi\sqrt{2C_{1eff}\beta}} \quad (36)$$

$$f_4 = \frac{\sqrt{4C_{1eff} + C_2}}{2\pi\sqrt{2C_{1eff}C_2\varepsilon}} \quad (37)$$

$$f_5 = \frac{\sqrt{(2-\sqrt{2})C_{1eff} + C_2}}{2\pi\sqrt{C_{1eff}C_2\Delta}} \quad (38)$$

$$f_6 = \frac{\sqrt{(2-\sqrt{2})C_{1eff} + C_2}}{2\pi\sqrt{C_{1eff}C_2\Delta}} \quad (39)$$

$$f_7 = \frac{\sqrt{(2+\sqrt{2})C_{1eff} + C_2}}{2\pi\sqrt{C_{1eff}C_2\gamma}} \quad (40)$$

$$f_8 = \frac{\sqrt{(2+\sqrt{2})C_{1eff} + C_2}}{2\pi\sqrt{C_{1eff}C_2\gamma}} \quad (41)$$

where

$$\alpha = L(1) + L(5) - 2L(3) + M(1) + M(5) - 2M(3) - M_{\text{end}}(1) - M_{\text{end}}(5) + 2M_{\text{end}}(3) \quad (42)$$

$$\beta = L(1) + L(5) + 2L(4) + 2L(3) + 2L(2) - M_{\text{end}}(1) - M_{\text{end}}(5) - 2M_{\text{end}}(4) - 2M_{\text{end}}(3) - 2M_{\text{end}}(2) \quad (43)$$

$$\varepsilon = L(1) + L(5) - 2L(4) + 2L(3) - 2L(2) + 2M(1) - 4M(4) + 2M(5) + 4M(3) - 4M(2) - M_{\text{end}}(1) - M_{\text{end}}(5) + 2M_{\text{end}}(4) - 2M_{\text{end}}(3) + 2M_{\text{end}}(2) \quad (44)$$

$$\Delta = 2L(1) - 2L(5) + 2(M(1) + M(4) - M(5) - M(2) - M_{\text{end}}(1) + M_{\text{end}}(5)) + \sqrt{2}(-2L(4) + 2L(2) - M(1) - 2M(4) + M(5)) + 2\sqrt{2}(M(2) + M_{\text{end}}(4) - M_{\text{end}}(2)) \quad (45)$$

$$\gamma = 2L(1) - 2L(5) + 2(M(1) + M(4) - M(5) - M(2) - M_{\text{end}}(1) + M_{\text{end}}(5)) + \sqrt{2}(2L(4) - 2L(2) + M(1) + 2M(4) - M(5)) - 2\sqrt{2}(M(2) + M_{\text{end}}(4) - M_{\text{end}}(2)) \quad (46)$$

Table 4 The frequencies calculated from the closed-form solutions obtained via the circulant formalism

i	1	2	3	4	5	6	7	8
f_i (MHz)	63.42	63.42	63.94	63.94	64.26	64.26	64.66	76.01

Table 3 The value of the self and mutual inductances used in the model and calculated via numerical integration

i	1	2	3	4	5
$L(i)$ (nH)	62.8	10.2	0.285	-2.61	-3.48
$M_{\text{end}}(i)$ (nH)	3.26	2.21	0.0434	-1.73	-2.39
$M(i)$ (nH)	215	50.4	31.6	24.7	22.7

The solutions presented have an automatic degeneracy of f_1 with f_2, f_5 with f_6 , and f_7 with f_8 . Table 3 contains values for the inductances that were calculated via numerical integration.

Using these values for the inductances together with $C_1=C_3=59.8$ pF and $C_2=49.2$ pF, the normal mode frequencies

were found. These results are displayed in Table 4. Note that there are three pairs of exactly degenerate modes and seven of the eight modes are 'nearly' degenerate due to the choices of C_1 and C_2 .

References

- Hayes CE, Edelstein WA, Schenck JF, Mueller OM, Eash M (1985) An efficient, highly homogeneous radiofrequency coil for whole-body NMR imaging at 1.5-T. *J Magn Reson* 63:622–628
- Jin J (1999) *Electromagnetic analysis and design*. CRC, New York
- Chin C-L, Collins C, Li S, Dardzinski B, Smith M (2002) Birdcage-builder: design of specified-geometry birdcage coils with desired current pattern and resonant frequency. *Magn Reson Eng* 15:156–163
- Tropp J (1992) The hybrid bird cage resonator. In: *Proceedings of the 11th Annual Meeting of the Society of Magnetic Resonance in Medicine, Society for Magnetic Resonance in Medicine*, p 4009
- Leussler C, Stimma J, Roschmann P (1997) The bandpass birdcage resonator modified as a coil array for simultaneous MR acquisition. In: *ISMRM Fifth Meeting Proceedings*, April 12–18, 1997, Vancouver, B.C., Canada, International Society for Magnetic Resonance in Medicine, p 176
- Leifer MC (1997) Resonant mode of the birdcage coil. *J Magn Reson* 124:51–60
- Eagan T, Chmielewski T, Flock J, Cheng Y, Kidane T, Shvartsman Sh, DeMeester G, Dannels W, Brown R (2002a) Understanding approximately degenerate eigenmodes in two-ring and three-ring RF birdcages. In: *Proceedings of the ISMRM Tenth Scientific Meeting and Exhibition, Honolulu, Hawaii, USA, May 18–24, 2002, International Society for Magnetic Resonance in Medicine*, p 164
- Eagan T, Cheng Y-C, Kidane T, Shvartsman S, Brown R (2002b) RF eigenmodes: Circulant theory and matrix applications. In: *Proceedings of the ISMRM Tenth Scientific Meeting and Exhibition, Honolulu, Hawaii, USA, May 18–24, 2002, International Society for Magnetic Resonance in Medicine*, p 873
- Pruessmann KP, Weiger M, Scheidegger MB, Boesiger P (2000) SENSE: sensitivity encoding for fast MRI. *Magn Reson Med* 42:952–962
- Sodickson DK, Manning WJ (1997) Simultaneous acquisition of spatial harmonics (SMASH): fast imaging with radiofrequency coil arrays. *Magn Reson Med* 38:591–603
- Willig-Onwuachi JD (2001) Field optimization in magnetic resonance imaging: Striving for perfect shielding and perfect sinusoids, Ph.D. thesis, Case Western Reserve University, Cleveland, Ohio
- Willig J, Brown R, Eagan T, Shvartsman S (2001) Birdcage-like coils for perfectly sinusoidal SMASH fields. In: *Syllabus of the ISMRM workshop on MRI hardware in Cleveland 2001, International Society for Magnetic Resonance in Medicine, Cleveland, Ohio, USA*
- J. Willig, R. Brown, T. Eagan, S. Shvartsman (2001) Perfectly sinusoidal SMASH field shapes from birdcage sectors. In: *Proceedings of the ISMRM ninth scientific meeting and exhibition, Glasgow, Scotland, UK, April 21–27, 2001, International Society for Magnetic Resonance in Medicine*
- Roemer PB, Edelstein WA, Hayes CE, Souza SP, Mueller OM (1990) The NMR phased array. *Magn Reson Med* 16:192–225
- Reykowski A, Wright SM, Porter J (1995) Design of matching networks for low noise preamplifiers. *Magn Reson Med* 33:848–852
- Lee RF, Giaquinto RO, Hardy CJ (2002) Coupling and decoupling theory and its application to the MRI phased array. *Magn Reson Med* 48:203–213
- Duensing GR, Peterson DM, Beck B, Fitzsimmons JR (2000) Transmission field profiles for transceive phased array coils. In: *Proceedings of the ISMRM Eighth Scientific Meeting and Exhibition, Denver, Colorado, USA, April 1–7, 2000, International Society for Magnetic Resonance in Medicine*, p 143
- Jevtic J (2001) Ladder networks for capacitive decoupling in phased-array coils. In: *Proceedings of the ISMRM ninth scientific meeting and exhibition, Glasgow, Scotland, UK, April 1–7, 2001*
- Gradshteyn IS, Ryzhik IM (2000) *Table of integrals, series, and products*. 6th edn. Academic, San Diego
- Grover FW (1946) *Inductance calculations*. D. Van Norstrand, New York